

Atomistic model of plutonium

M. I. Baskes

Los Alamos National Laboratory, Los Alamos, New Mexico 87545

(Received 31 May 2000; revised manuscript received 7 August 2000)

A modified embedded atom model of Pu has been developed. This simple atomic level model is able to reproduce the extreme anomalous behavior of this complex element. The calculated energetics and volume of the seven stable phases of Pu are found to be in close agreement with experiment. Calculated thermodynamic and elastic properties are also in reasonable agreement with the available experimental data. The model also reproduces the unusual properties of the liquid phase, low melting point, and contraction upon melting. It is demonstrated that the anomalous properties of plutonium arise from the rapid spatial variation of the f -electron density.

I. INTRODUCTION

Plutonium is perhaps the most complex of all elements. Its phase diagram shows the existence of six equilibrium solid phases as well as the liquid phase at atmospheric pressure. No other element possesses this complexity of polymorphism. Most unusual is the extreme variation in atomic volume found in plutonium. The close-packed fcc phase is found to have the *largest* volume per atom of all of its phases. Plutonium melts at a temperature much lower than its neighbors in the Periodic Table and does so with a decrease in volume, unlike the vast majority of materials. Of course, in addition to its unusual properties, plutonium is of great technological importance due to its use in nuclear weapons. Modern day problems concerning plutonium involve predicting its properties under long-term aging in both a weapons¹ and storage environment.² Development of a predictive aging model for plutonium is a major goal of the Stockpile Stewardship Program of the DOE. Such predictions require an atomic level model, which until now did not exist.

Recent research has led to a model of a similarly complex element, tin.³ This model was based on the embedded atom method⁴⁻⁶ (EAM) that has been found to represent the properties of metals and alloys quite well. The EAM, which is based on density-functional theory, is by far the most widely used semiempirical atomistic method. Applications of the EAM include calculations of properties of perfect and defective (free surfaces, point defects, grain boundaries, dislocations, etc.) bulk metals and alloys as a function of temperature and pressure. In the work on tin it was found that the model was able to quantitatively predict the thermodynamics of the three equilibrium phases of tin. The addition of angular forces⁷ was found to be critical in explaining the behavior of complex crystal structures.

The phases of plutonium

In Fig. 1, the stable phases of plutonium are depicted. At lower temperatures two distinct monoclinic phases, α and β , are found. Higher-temperature phases include a severely distorted (orthorhombic) diamond cubic phase γ ; the fcc phase δ ; a tetragonal distortion of the fcc phase δ' ; the bcc phase ϵ ; and finally, the liquid phase. Over a range of temperature

of only 900 K, the internal energies of these phases vary by only about 0.4 eV atom and the volume per atom varies by about 25%.⁸

II. THEORY

A. Details of the model

The total energy E of a system of monatomic atoms in the EAM has been shown⁴⁻⁶ to be given by an approximation of the form

$$E = \sum_i \left(F(\bar{\rho}_i) + \frac{1}{2} \sum_{j \neq i} \phi(R_{ij}) \right), \quad (1)$$

where the sums are over the atoms i and j . In this approximation, the embedding function F is the energy to embed an atom of type i into the background electron density at site i , $\bar{\rho}_i$; and ϕ is the pair interaction between atoms i and j whose separation is given by R_{ij} . In the EAM, $\bar{\rho}_i$ is given by a linear superposition of spherically averaged atomic electron densities, while in the modified embedded atom method (MEAM), $\bar{\rho}_i$ is augmented by angularly dependent terms.^{7,9,10}

The pair potential between two atoms $\phi(R)$ separated by a distance R is given by

$$\phi(R) = \frac{2}{Z} \{ E^u(R) - F[\bar{\rho}^0(R)] \}, \quad (2)$$

where $\bar{\rho}^0(R)$ is the background electron density at an atom in what we call the reference structure, and Z is the number of first neighbors in this structure. Here, $E^u(R)$ is the energy per atom of the reference structure as a function of nearest-neighbor distance R , obtained, e.g., from first-principles calculations or the universal equation of state of Rose *et al.*¹¹ Here we choose a slightly modified form of the latter:

$$E^u(R) = -E_c \left(1 + a^* + \delta a^{*3} \frac{r_e}{R} \right) e^{-a^*}, \quad (3)$$

with

$$a^* = \alpha \left(\frac{R}{r_e} - 1 \right) \quad (4)$$

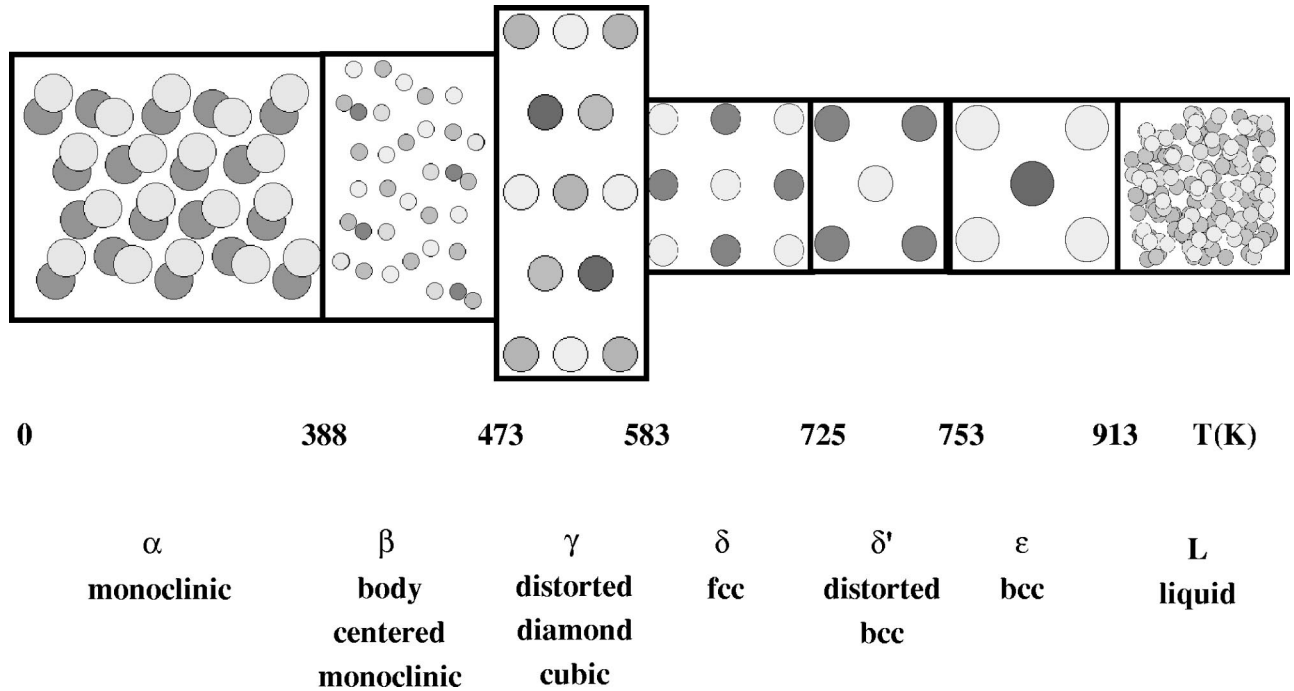


FIG. 1. The stable phases of plutonium at atmospheric pressure. Each phase is schematically shown in the temperature region over which it is stable. Shading represents atoms at different depth. The c planes shown for the α phase show a distorted sixfold coordination around each atom reminiscent of the (111) planes in the fcc structure. The γ phase results from a large orthorhombic distortion of the diamond cubic phase.

and

$$\alpha^2 = \frac{9\Omega B}{E_c}, \quad (5)$$

where E_c , r_e , Ω , and B are the cohesive energy, nearest-neighbor distance, atomic volume, and bulk modulus, respectively, all evaluated at equilibrium in the reference structure. The cubic term in a^* is a small correction with strength δ , which was found to be important for the dense α -Pu phase and is directly related to the pressure derivative of the bulk modulus. Thus, as discussed below, the parameter δ has been chosen by using the experimental value for the pressure derivative for the α phase. In this work, the reference structure will be taken as fcc, resulting in

$$\bar{\rho}^0(R) = Z\rho^{a(0)}(R), \quad (6)$$

where $\rho^{a(0)}$ is an atomic electron density discussed below.

In the MEAM, the embedding function $F(\bar{\rho})$ is taken as

$$F(\bar{\rho}) = AE_c \frac{\bar{\rho}}{\rho_0} \ln \frac{\bar{\rho}}{\rho_0}, \quad (7)$$

where A is an adjustable parameter and ρ_0 is a density-scaling parameter. For the fcc reference structure $\rho_0 = Z = 12$.

The background electron density at a specific site $\bar{\rho}$ is assumed to be a function of what we call partial electron densities. These partial electron densities contain the angular information in the model. The spherically symmetric partial electron density $\rho^{(0)}$ is the background electron density in the EAM:

$$\rho^{(0)} = \sum_i \rho^{a(0)}(r^i), \quad (8)$$

where the sum is over all atoms i not including the atom at the specific site of interest and r^i is the distance from an atom i to the site of interest. The angular contributions to the density are given by similar formulas weighted by the x , y , and z projections of the distances between atoms.⁷ The atomic electron densities are taken to be simple exponentials with decay constant $\beta^{(l)}$, $l=0-3$. To obtain the background electron density from the partial electron densities, we make the assumption that the angular terms are a small correction to the EAM. We combine the angular dependence into one term:

$$\Gamma = \sum_{l=1}^3 t^{(l)} (\rho^{(l)}/\rho^{(0)})^2, \quad (9)$$

where $t^{(l)}$ are constants. The background density is then taken as

$$\bar{\rho} = \rho^{(0)} \sqrt{1 + \Gamma}. \quad (10)$$

It has been shown that this formalism is equivalent to an expansion of the background electron density in Legendre polynomials.^{7,12}

B. Obtaining the model parameters

The MEAM parameters are obtained by using literature experimental data for plutonium and a gallium-stabilized plutonium alloy. In Table I, the source of the experimental data for each parameter, as well as the resultant parameter value, is given. The experimental data used includes the co-

TABLE I. Source and values of MEAM parameters for plutonium. Where appropriate experimental data was not available, nominal values were chosen that are similar to the values used for other elements.

Parameter	Source	Value
E_c (eV)	cohesive energy of the liquid ^a	3.80
r_e (Å)	lattice constant of δ^a	3.28
α	bulk modulus of Ga-stabilized δ^b	3.31
A	relative energy of δ and ϵ^a	1.05
$\beta^{(0)}$	shear modulus of Ga-stabilized δ^b	2.39
$\beta^{(1)}$	nominal value	1.0
$\beta^{(2)}$	nominal value	6.0
$\beta^{(3)}$	volume per atom of α^a	9.0
$t^{(1)}$	nominal value	1.0
$t^{(2)}$	shear modulus of Ga-stabilized δ^b	4.14
$t^{(3)}$	relative energy of δ and α^a	-0.8
δ	pressure derivative of bulk modulus of α^c	0.46

^aReference 8.

^bReference 24.

^cReference 25.

hesive energy of liquid plutonium, the lattice constant of fcc δ -Pu, the elastic constants of a gallium-stabilized fcc plutonium alloy, the volume per atom and pressure derivative of the bulk modulus of monoclinic α -Pu, and the heats of transformation between various allotropes of plutonium. Even though the parameters are not completely uncorrelated, there is a very close connection between each piece of experimental data and the resultant parameter. For three parameters, no appropriate experimental data is available. In these cases a nominal value has been chosen. These values are consistent with values used in the modeling of other elements.⁷ Detailed effects of this choice have not been evaluated. Quantitative agreement with experiment may be obtained for a range of these parameters. Angular screening was implemented using standard values, $C_{\min}=2.0$ and $C_{\max}=2.8$, in the method of Baskes, Angelo, and Bisson.¹³ For computational convenience, a radial cutoff of 4.5 Å was also used.¹⁴ It should be noted that in models that use angular screening, in contrast to the conventional models that use only a radial cutoff, the value of the radial cutoff is unimportant. Specifically, for essentially all atom configurations, the range of the functions is limited by the angular screening, not the radial cutoff. It should also be noted that the inclusion of angular forces in the EAM makes the inclusion of long-range interactions unnecessary. In the MEAM phase stability (even fcc/hcp) is determined by nearest-neighbor interactions. The choice of radial cutoff does not significantly affect any of the results presented here.

C. Computational details

The calculations presented below used the molecular dynamics technique. Typically, the calculations used a three-dimensional periodic cell of ~ 250 atoms with dynamic periodic boundaries.¹⁵ The melting calculations used a cell of 1000 atoms. For these calculations the angle in the monoclinic structures was held fixed at the experimental value. Temperature was controlled using a standard Nose-Hoover

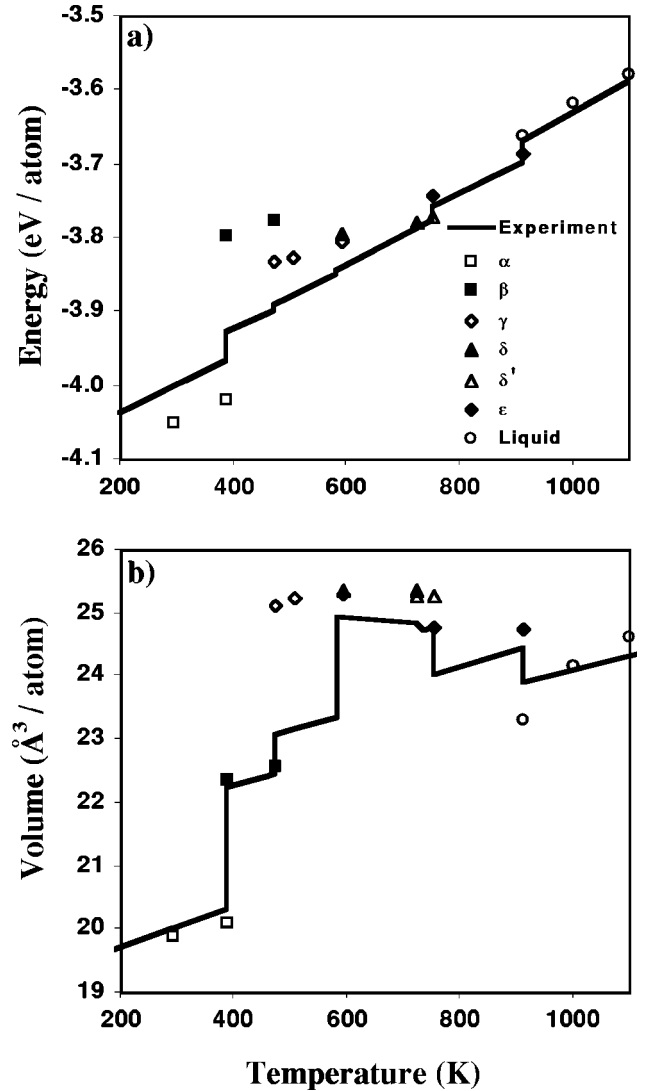


FIG. 2. Comparison of the calculated and experimental energy (a) and volume (b) of the equilibrium plutonium phases as a function of temperature. The energies are relative to isolated, noninteracting atoms at infinity. The data are shown over the experimental regions of stability. The monoclinic angles for the α and the β phases were held fixed at the experimental values.

thermostat^{16,17} with a time constant of 0.1 ps. The quantities reported below are thermodynamic averages for over at least 10 ps from samples that had been equilibrated at temperature and pressure for at least 10 ps. Statistical errors in energy are less than 10 meV/atom and in volume, less than 0.2 Å³/atom. Average pressures were typically <100 MPa, and average temperatures were typically within <1 K of the desired temperature.

III. RESULTS AND DISCUSSION

A. How the model compares to experiment

In Fig. 2(a), the energetics of the allotropes are compared to experiment. We see that the relative order of the phases, as predicted by the MEAM model, is almost identical to that expected from the experiment. The energy of the liquid is close to the experimental value of -3.5 eV/atom at ~ 1600 K.⁸ The predicted β -phase energy appears to be a bit high.

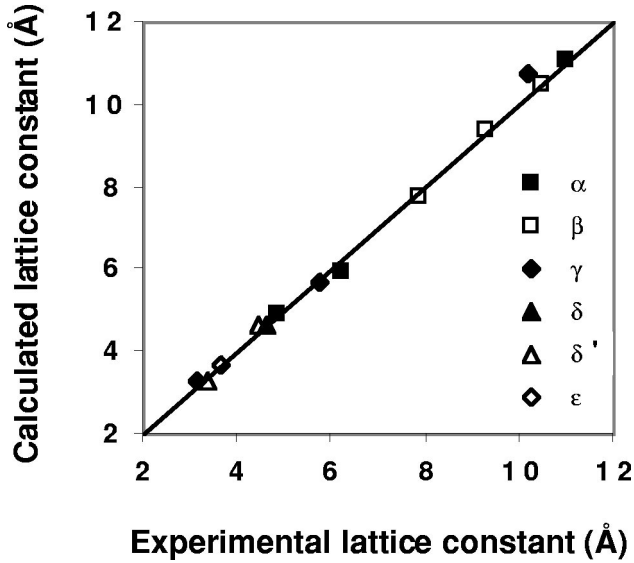


FIG. 3. Comparison of the calculated and experimental lattice constants of the equilibrium plutonium allotropes. The data are shown for the following temperatures: α , 294 K; β , 463 K; γ , 508 K; δ , 593 K; δ' , 738 K; and ϵ , 763 K. The three widely separated lattice constants show the large orthorhombic distortion of the diamond cubic phase.

The predicted slopes (heat capacity) of the liquid, α , and ϵ phases are in reasonably good agreement with experiment. In contrast, the slopes for the other phases are significantly lower than the experimental slopes, possibly indicating that electronic effects, which are not directly included in the MEAM, could be important (see Wallace¹⁸ for a discussion of the relative importance of anharmonic and electronic effects in plutonium). The enthalpy changes due to the phase transformations are in good agreement with experiment. In Fig. 2(b), the volumes of the allotropes are compared to experiment. We see that the unusual behavior in plutonium is well reproduced by the model. The close-packed fcc δ phase has the highest volume per atom of all of the phases. We see that the γ phase takes on a volume reminiscent of the δ phase rather than the β phase as seen in experiment. Preliminary results show that variation of the monoclinic angle in the α and β phases does not change the equilibrium energy or volume significantly. The slopes of the curves (thermal expansion) are in reasonable agreement with experiment. The experimentally observed negative thermal expansion of the δ and δ' phases is not reproduced, but these phases are predicted to have thermal expansion coefficients much lower than the other phases. The model shows a decrease in volume upon melting, as seen in experiment. The calculated melting point is found to be about 1000 K, in reasonable agreement with the experimental melting point of 913 K. Melting points are calculated using the moving planar interface method.¹⁹ Not only does the model reproduce the experimental volumes, but the lattice constants of the crystalline phases are also in excellent agreement with experiment (Fig. 3). Most notable is the agreement with experiment of the lattice constants of the γ phase, which may be considered as a very significant orthorhombic distortion of the diamond cubic structure. The predicted elastic moduli are compared to experiment in Table II. The moduli are obtained from a fit of the calculated pressure/volume relationship to a second-order

TABLE II. Elastic moduli for plutonium. Calculated values of the bulk modulus B and pressure derivative of the bulk modulus B' . Experimental values are given in parentheses.

Phase	T (K)	B (GPa)	B' (dimensionless)
α	294	41 (40–48 ^a , 42 ^b)	11 (10.5 ^b)
β	388	31 (30–43 ^c)	7.4
γ	508	23 (23 ^d)	17
δ	593	25 (41 ^e)	5.7
ϵ	913	21	2.2
liquid	1100	7.9	0.1

^aReference 26 at 303 K.

^bReference 25.

^cReference 27 at 473 K.

^dReference 8 at 493 K.

^eReference 8 at 603 K.

polynomial in the logarithm of volume over volume variations of about 5%. Reasonable agreement with experiment is obtained. The anomalously high-pressure derivative of the bulk modulus for the α phase is reproduced well by the model. It should be emphasized that the pressure derivative was fit to experiment and is *not* a prediction of the model.

B. Understanding the complex behavior

By looking at the details of the model, we can begin to develop an understanding of why plutonium has such an unusual behavior. In comparing the model parameters to those for other materials,^{7,20} only one parameter stands out as being different, $\beta^{(3)}$, the decay constant for the f -electron density. This constant is much larger for plutonium than any other element that has been modeled using the MEAM. What this means is that the f -electron density has a much more rapid spatial variation than the s -, p -, or d -electron densities. This variation allows the bonding in plutonium at a large atomic volume to be mainly s in character, while at small atomic volumes, to be mainly f in character. Here we equate the mathematical concept of partial electron density described above to the more physical concept of bonding character. The reader is cautioned that connecting the concepts of the empirical MEAM with electronic structure theory should be viewed with caution. These ideas are consistent with those proposed by Zachariasen many years ago,²¹ and recent density-functional calculations.^{22,23} We can quantify these concepts from our calculations. In Table III, the average ratios of the p , d , and f partial electron densities to the

TABLE III. Average ratio of the l ($l=p,d,f$) component of the electron density to the s component $\chi = \rho^{(l)}/\rho^{(0)}$ for the various phases at the indicated temperature. The densities were sampled at times spaced by 0.02 ps over a 5 ps duration.

Phase	T (K)	p	d	f
α	294	0.05	0.10	0.78
β	473	0.09	0.13	0.35
γ	508	0.05	0.07	0.13
δ	593	0.05	0.07	0.11
ϵ	913	0.08	0.11	0.20
liquid	913	0.10	0.16	0.50

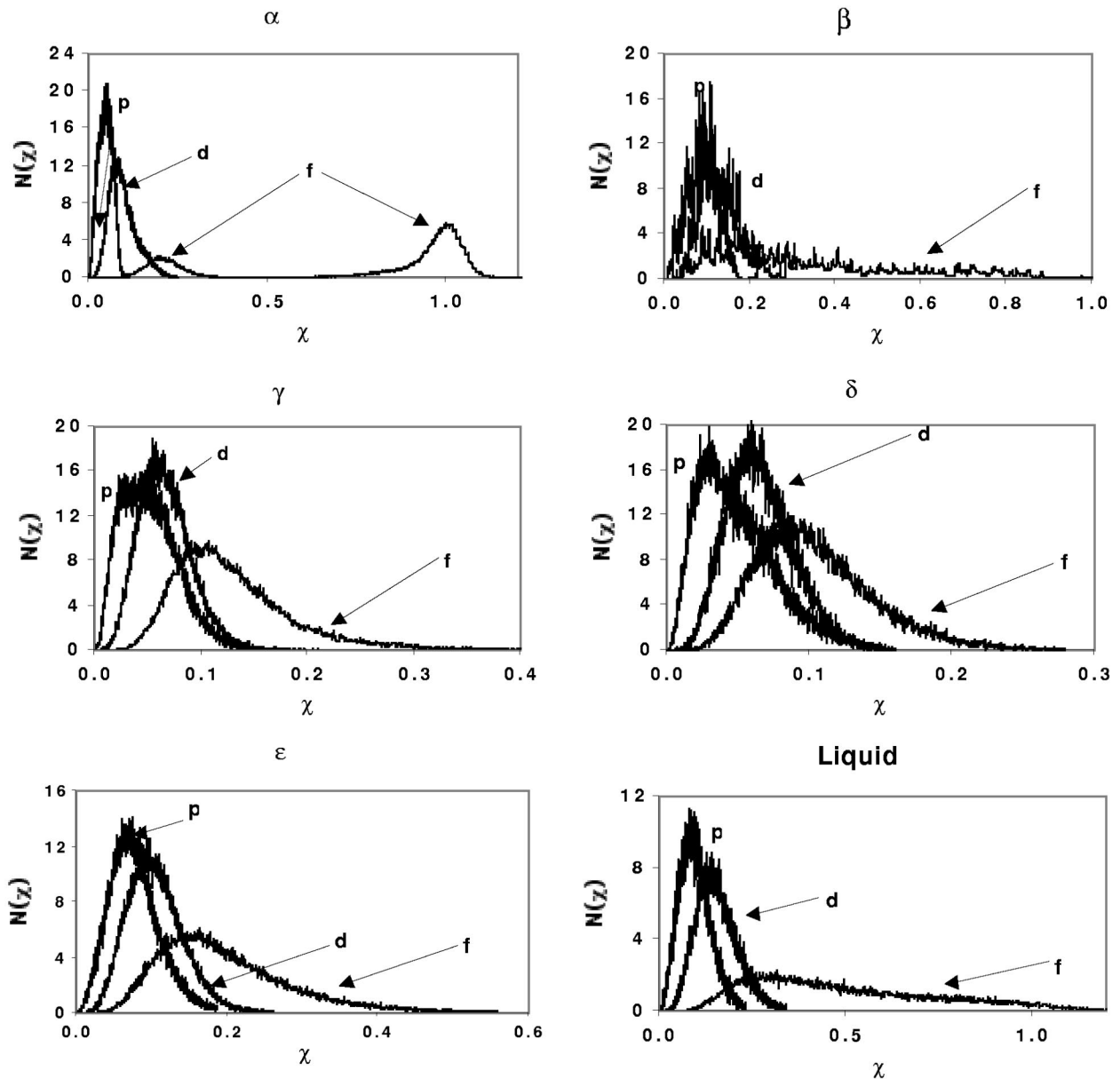


FIG. 4. Distribution function $N(\chi)$ of the ratio of the l ($l=p, d, f$) component of the electron density to the s component $\chi = \rho^{(l)}/\rho^{(0)}$ for various phases of plutonium. Note the different scales for the different phases. The data were collected for the temperatures presented in Table III. The distribution (1000 bins, normalized to unity) includes ratios for all atoms at times spaced by 0.02 ps over a 5 ps duration. The peak widths are due to both the random motion of the neighbors of each atom caused by temperature and also the different average environments seen by atoms in these complex crystal structures. For example, in the α phase there are three environments that contribute to the f electron density peaks. Atoms from the first environment contribute to the peak at ~ 0.2 , atoms from the second environment contribute to the peak at ~ 1.0 , while atoms from the third environment contribute to the shoulder of the large peak at ~ 0.8 .

s -electron density are presented. The average is taken over both the atoms and time. We posit that these ratios are representative of the extent of the bonding of electrons with different angular momentum states. The average electron density for the p electrons ranges from 5% to 10% of the s -electron density, increasing from the low-temperature α phase to the high-temperature liquid. The β phase violates this trend. The d -electron density varies from 7% to 16% of the s -electron density with no apparent systematic variation between the phases. The most dramatic variation occurs for the f -electron density, which ranges from 11% of the s -electron density in the δ phase to 78% of the s -electron density in the α phase. Clearly, the bonding in these two

phases is drastically different. We can understand the source of this behavior in Fig. 4 where we show the distribution of the electron-density ratios. The figure presents distribution functions of the ratios collected for all of the atoms and for a time of 5 ps. For all of the phases, this ratio for the p and d electrons is small, approximately Gaussian in shape, and peaks at ratios between 5% and 20%, consistent with the averages shown in Table III. The spread in ratios may be attributed to the changes in environment that an atom sees due to thermal vibration. In contrast, the ratio for the f electrons varies significantly from phase to phase. It is the smallest for the δ phase, the phase with the largest volume per atom and shows a bimodal distribution for the α phase, the

phase with the smallest volume per atom. Detailed investigation shows that about $\frac{2}{3}$ of the atoms in the α phase contribute to the peak that represents approximately equal s and f electron density. The β and liquid phases show a significant amount of f -bonding character, while the γ and ϵ phases show only slightly more f bonding than the δ phase. Thus, we are able to conclude that the large volume per atom of the cubic δ and ϵ phases arises from plutonium atoms with predominantly s -like bonding, and the smaller volume per atom of the monoclinic α and β phases results from plutonium atoms with a high degree of f -like bonding.

IV. FUTURE DIRECTIONS

To ensure that our model represents the properties of plutonium, we plan to calculate a number of additional proper-

ties, e.g., all of the elastic constants and self-diffusion, for which there is experimental data to compare. In addition, two extensive sets of calculations are planned for elemental plutonium. The first involves calculation of the free energies of all of the stable phases so that transformation temperatures may be predicted and compared to experiment. The second involves calculation of radiation damage in the delta phase so that the long-term stability of this material may be assessed. Assuming that these tests yield positive results, the logical extension of the model is to include common alloying additions, e.g., gallium, and important impurities, e.g., helium. With the addition of a model for these elements, we should be able to calculate the entire plutonium/gallium phase diagram, including the effects of the important plutonium decay product, helium.

-
- ¹S. Drell, R. Jeanloz, and B. Peurifoy, *Science* **283**, 1119 (1999).
²W. K. H. Panofsky, *Science* **275**, 11 (1997).
³R. Ravelo and M. Baskes, *Phys. Rev. Lett.* **79**, 2482 (1997).
⁴M. S. Daw and M. I. Baskes, *Phys. Rev. Lett.* **50**, 1285 (1983).
⁵M. S. Daw and M. I. Baskes, *Phys. Rev. B* **29**, 6443 (1984).
⁶M. S. Daw, S. M. Foiles, and M. I. Baskes, *Mater. Sci. Rep.* **9**, 251 (1993).
⁷M. I. Baskes, *Phys. Rev. B* **46**, 2727 (1992).
⁸O. J. Wick in *Plutonium Handbook: A Guide to the Technology* (The American Nuclear Society, La Grange Park, IL, 1980), Vols. I and II.
⁹M. I. Baskes, *Phys. Rev. Lett.* **59**, 2666 (1987).
¹⁰M. I. Baskes, J. S. Nelson, and A. F. Wright, *Phys. Rev. B* **40**, 6085 (1989).
¹¹J. H. Rose, J. R. Smith, F. Guinea, and J. Ferrante, *Phys. Rev. B* **29**, 2963 (1984).
¹²M. I. Baskes, *Mater. Sci. Eng., A* **261**, 165 (1999).
¹³M. I. Baskes, J. E. Angelo, and C. L. Bisson, *Modell. Simul. Mater. Sci. Eng.* **2**, 505 (1994).
¹⁴M. I. Baskes, *Mater. Chem. Phys.* **50**, 152 (1997).
¹⁵M. Parrinello and A. Rahman, *J. Appl. Phys.* **52**, 7182 (1981).
¹⁶W. G. Hoover, *Phys. Rev. A* **31**, 1695 (1985).
¹⁷S. Nose, *Prog. Theor. Phys. Suppl.* **103**, 1 (1991).
¹⁸D. C. Wallace, *Phys. Rev. B* **58**, 15 433 (1998).
¹⁹M. I. Baskes, *Phys. Rev. Lett.* **83**, 2592 (1999).
²⁰M. I. Baskes and R. A. Johnson, *Modell. Simul. Mater. Sci. Eng.* **2**, 147 (1994).
²¹W. H. Zachariasen, in *The Metal Plutonium*, edited by A. S. Coffinberry and W. N. Miner (University of Chicago Press, Chicago, 1961), p. 99.
²²J. van Ek, P. A. Sterne, and A. Gonis, *Phys. Rev. B* **48**, 16 280 (1993).
²³P. Söderlind, J. M. Wills, B. Johansson, and O. Eriksson, *Phys. Rev. B* **55**, 1997 (1997).
²⁴H. M. Ledbetter and R. L. Moment, *Acta Metall.* **24**, 891 (1976).
²⁵R. B. Roof, in *Compression and Compressibility Studies of Plutonium and a Plutonium-Gallium Alloy*, edited by D. K. Smith, C. Barrett, D. E. Leyden, and P. K. Predecki (Plenum, New York, 1981), Vol. 24, p. 221.
²⁶H. L. Laquer, in *Sound-Velocity Measurements on Alpha-Phase Plutonium*, edited by A. S. Coffinberry and W. N. Miner (University of Chicago Press, Chicago, 1961), p. 157.
²⁷A. S. Coffinberry and M. B. Waldron, in *The Physical Metallurgy of Plutonium*, edited by H. M. Finnieston and J. P. Howe (McGraw-Hill, New York, 1956), Vol. 1, p. 382.